SP-B and SP-C Alter Diffusion in Bilayers of Pulmonary Surfactant

Vincent Schram and Stephen B. Hall
Departments of Biochemistry and Molecular Biology, Medicine, and Physiology and Pharmacology, Oregon Health & Science University, Portland, Oregon 97239-3098

ABSTRACT The hydrophobic proteins SP-B and SP-C promote rapid adsorption of pulmonary surfactant to an air/water interface by an unknown mechanism. We tested the hypothesis that these proteins accelerate adsorption by disrupting the structure of the lipid bilayer, either by a generalized increase in fluidity or by a focal induction of interfacial boundaries within the bilayer. We used fluorescence recovery after photobleaching to measure diffusion of nitrobenzoxadiazolyl-dimyristoyl-phosphatidylethanolamine between 11 and 54°C in multilayers containing the complete set of lipids and proteins in calf lung surfactant extract (CLSE), or the complete set of neutral and phospholipids without the proteins. Above 35°C, Arrhenius plots of diffusion were parallel for CLSE and neutral and phospholipids, but shifted to lower values for CLSE, suggesting that the proteins rigidify the lipid bilayer rather than producing the proposed increase in membrane fluidity. The slopes of the Arrhenius plots for CLSE were steeper below 35°C, suggesting that the proteins induce phase separation at that temperature. The mobile fraction fell below 27°C, consistent with a percolation threshold of coexisting gel and liquid-crystal phases. The induction of lateral phase separation in CLSE, however, does not correlate with apparent changes in adsorption kinetics at this temperature. Our results suggest that SP-B and SP-C accelerate adsorption through a mechanism other than the disruption of surfactant bilayers, possibly by stabilizing a high-energy, highly curved adsorption intermediate.

INTRODUCTION

Small amounts of hydrophobic proteins specific to pulmonary surfactant are essential for its function. Lung surfactant forms a thin film at the air/water interface in the alveolus, thereby reducing the tendency of surface tension to collapse the lungs. The hydrophobic surfactant proteins, SP-B and SP-C, promote adsorption of surfactant vesicles to form the interfacial film. Surfactant lipids, whether the complete set (Wang et al., 1996) or simple model systems (Whitsett et al., 1986; Hawgood et al., 1987; Warr et al., 1987; Arjomaa and Hallman, 1988; Yu and Possmayer, 1990; Oosterlaken-Dijksterhuis et al., 1991), adsorb slowly without the proteins. Babies (Nogee, 1998) and animals (Tokieda et al., 1997) that lack these proteins because of genetic defects die from respiratory failure.

The studies reported here address potential mechanisms by which the proteins might facilitate adsorption. These mechanisms follow directly from the earliest models of surfactant function that were conceived before the existence of the hydrophobic surfactant proteins was recognized. Relative to the phospholipids in other biological systems, pulmonary surfactant contains an unusually large fraction of the fully saturated compound dipalmitoyl phosphatidylcholine (DPPC), which at physiological temperatures remains below its gel-to-liquid crystal melting transition. Artificially spread films containing only DPPC replicate the essential ability of surfactant films in situ to sustain surface pressures well above equilibrium values. Vesicles of DPPC, however, adsorb to the surface quite slowly. Original theories held that the ability of DPPC to form highly ordered, rigid structures resulted in its stability at the interface, but also in its slow transformation from bilayer vesicles to surface film. The other constituents were thought to function by disruption of the ordered bilayers, producing more fluid structures that could adsorb more rapidly to form the interfacial film (Notter, 1984; Keough, 1985).

Measurement of fluorescence recovery after photobleaching (FRAP) is one method commonly used to determine the fluidity of a bilayer. For a bilayer labeled with a fluorescent probe soluble only in the liquid-crystal phase, the rate at which fluorescence recovers following photobleaching of a limited area provides D, the diffusion coefficient of the probe (Vaz, 1994). Because translational diffusion measured by FRAP is inversely related to viscosity, measurements of D provide information on the rheological characteristics of the liquid-crystal phase.

FRAP can also provide information concerning a second mechanism by which the proteins may promote adsorption. Rather than causing a generalized disorder throughout the bilayer, the proteins could produce a more focal effect by inducing phase separation of the surfactant lipids. The discontinuous change in lipid packing at the linear interface between two phases represents a region of concentrated defects in the bilayer structure. The suggestion that interfacial boundaries provide a particularly favorable site for the fusion of two bilayers (Leckband et al., 1993) raises the possibility that they may also favor the fusion of a surfactant vesicle either with an air/water interface or with a preexisting surface monolayer (Gugliotti and Politi, 2001). The proteins could lengthen interfacial boundaries between phases within the

Submitted November 25, 2003, and accepted for publication February 3, 2004.

Address reprint requests to Stephen B. Hall, Molecular Medicine, M/C NRC-3 OHSU, Portland, OR 97239-3098. E-mail: sbh@ohsu.edu.

0006-3495/04/06/3734/10 $2.00

doi: 10.1529/biophysj.103.037630

vesicle either by shifting the phase diagram to alter the amounts of coexisting phases, or by lowering line tension and extending the interfacial perimeter. Studies with monolayers of pulmonary surfactant provide precedence for both effects. The proteins alter the extent of coexisting phases and also the distribution of the more condensed phase into individual domains, thereby extending the length of the interfacial boundary (Discher et al., 1999). Because a phase in which the probe is insoluble acts as an obstacle to its diffusion, FRAP is sensitive to both the extent of phase separation and the configuration of the coexisting phases (Vaz et al., 1985a; Bultmann et al., 1991; Almeida et al., 1992a; Saxton, 1992; Schram and Thompson, 1995; Schram et al., 1996). FRAP therefore provides an appropriate method for investigating the previously untested possibility that the proteins promote adsorption by causing extended interfacial boundaries.

Our experiments measure FRAP of *N*-(7-nitrobenzoxa-2,3-diazol-4-yl)-dimyristoyl-phosphatidylethanolamine (NBD-DMPE) to determine the effect of the surfactant proteins on both the rheology and the phase behavior of stacked bilayers containing the surfactant lipids. Our studies use the complete set of lipids from calf surfactant with or without physiological levels of the proteins SP-B and SP-C to maximize the relevance of our results. Experiments over a range of temperatures allow comparisons with previous measurements to determine if effects established by FRAP correlate with changes in adsorption rates.

MATERIALS AND METHODS

Materials

Dioleoyl phosphatidylcholine (DOPC), DPPC, and NBD-DMPE were obtained from Avanti Polar Lipids (Alabaster, AL) and used without further characterization or purification. Extracted calf surfactant (Calf Lung Surfactant Extract, CLSE), obtained from ONY (Amherst, NY), was prepared as described previously (Notter et al., 1983). All other chemicals were of analytical grade. Solvents were of spectroscopic grade. Our standard buffer contained 150 mM NaCl, 1.5 mM $CaCl_2$, 10 mM Hepes, pH 7.0 (HSC).

The hydrophobic proteins were removed from CLSE by gel permeation chromatography (Hall et al., 1994). Pooled fractions that contain phospholipid or cholesterol provided the neutral and phospholipids (N&PL). This procedure reduces the protein content from 10 μg protein/μmol phospholipid for CLSE to undetectable levels below 0.5 μg/μmol in N&PL without altering the composition of phospholipid head groups or the cholesterol/phospholipid ratio (Hall et al., 1994).

Methods

Biochemical assays

Phospholipid concentrations were determined by phosphate assay (Ames, 1966). Protein content was assayed with amido black on material precipitated with trichloroacetic acid (Kaplan and Pedersen, 1989). Total cholesterol was assayed by reduction with ferrous sulfate (Searcy and Bergquist, 1960).

Gas chromatography

1 mg of dried lipid was saponified with alcoholic KOH at 37°C, esterified in 14% boron trifluoride/methanol for 10 min at 100°C and extracted with hexane. The fatty acid-methyl esters were then analyzed with gas-liquid chromatography on an instrument equipped with a hydrogen flame ionization detector (model Sigma 3B, Perkin-Elmer, Norwalk, CT) and a 30-m fused silica capillary column (Supelco, Bellefonte, PA). The temperatures of the column, detector, and injection ports were 195°C, 250°C, and 250°C, respectively. Helium was used as the carrier gas. A computer program (Turbochrom, Perkin-Elmer) measured the retention time and area of each peak. A mixture of fatty acid standards was run daily.

Multilayers

Supported multilayers were prepared according to standard protocols (Vaz et al., 1985a). Lipids in chloroform solution were mixed with 0.1% (mol/mol) fluorescent probe and vortexed extensively. Sequential droplets of the solution were deposited on a microscope slide heated at 50°C without allowing the deposit to spread over an area larger than 1 cm^2. The slides were then incubated at 50°C in a water-saturated atmosphere for 12 h before adding 50 μl of buffer and covering with a coverslip. After 6 additional h at 50°C, the coverslips were sealed with high-vacuum silicone grease and kept at 50°C overnight. Multilayers of CLSE and N&PL were obtained only when using HSC buffer, whereas best results were obtained for DOPC and DPPC by using Hepes 10 mM, pH 7.0 without other electrolyte. A limited number of control experiments on DOPC and DPPC multilayers that were successfully prepared in HSC showed no significant difference from samples prepared using low-salt buffer.

FRAP experiments

Fluorescence measurements used a custom-built apparatus (Fig. 1) that illuminated a uniform circular disk with 12 μm radius for photobleaching. The 488-nm line from an Argon laser operated at 250 mW was divided into a primary beam (97% intensity) used for photobleaching, and a secondary beam that was further attenuated by neutral density filters and used to monitor fluorescence recovery (0.01% intensity). Fast electronic shutters, actuated by computer using programs constructed with the graphical user interface LabVIEW (National Instruments, Austin, TX), controlled exposure of the sample to each beam. The separated beams were recombined by passage through a cube beam-splitter along a common pathway into the illumination port of an epifluorescence microscope (Fig. 1).

Fluorescence recoveries were analyzed according to previously published equations (Lopez et al., 1988) that combine expressions for short (Lardner, 1977) and long (Soumpasis, 1983) times. The mobile fraction M was defined as the fraction of probe free to diffuse, and measured as the extent of recovery extrapolated to infinite time (Lopez et al., 1988). Experimental recovery curves were fitted with the diffusional equation using a linear Levenberg-Marquardt algorithm available through LabVIEW. Because the photomultiplier tube was closed during bleaching, the initial fluorescence intensity immediately after bleaching was not measured but determined by back-extrapolation of the fluorescence recovery.

Measurements were made at a series of temperatures. The samples were regulated with a home-built thermostated stage to within $\pm$0.25°C. The sample was initially warmed to 54°C at a rate of 6°C/h and kept at 54°C for 1 h before cooling at approximately the same rate while measurements were taken. Cooling scans resulted in gel phase growing into the liquid-crystal phase and allowed domains of the new phase to grow under fewer constraints than during heating. At least 30 recoveries on three different samples were averaged for each condition.

RESULTS

Our experiments measured the translational diffusion of the fluorescent probe NBD-DMPE in multilayers containing complete CLSE or the complete set of N&PL obtained by

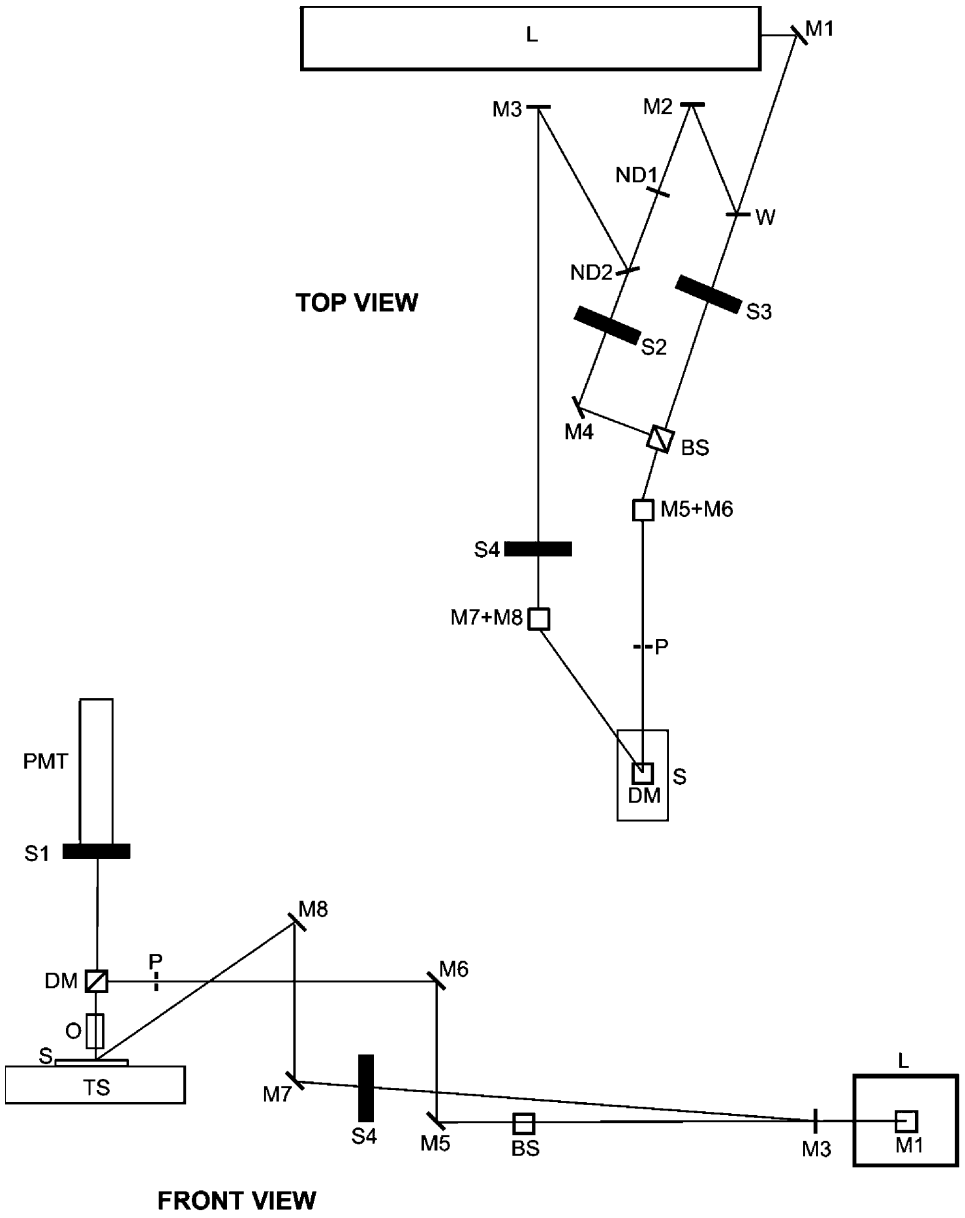

FIGURE 1 Schematic diagram of instrument for measuring FRAP. *Upper part*: view from above. *Lower part*: side view. The 488-nm line of an argon laser (*L*) is directed by mirrors (*M1*, *M2*,. . .*M8*) at an optical window (*W*) (BK7, Melles-Griot, Irvine, CA). The transmitted beam (97% intensity) is used for photobleaching, whereas the reflected beam (2% intensity) is further attenuated by 30× and 8× reflective neutral density filters (*ND1* and *ND2)* and used for monitoring fluorescence recovery. Fast electronic shutters (Vincent Associates, Rochester, NY) in the bleaching (*S3*) and monitoring (*S2*) beam paths control exposure of the sample to each beam. Bleaching and monitoring beams are recombined using a cube beam-splitter (BS, Melles-Griot, Irvine, CA) and directed into the epi-illuminator port of a multipurpose Zeiss ACS microscope (Zeiss, Oberkochen, Germany). The Gaussian intensity profile of the incident beam is converted into a quasisquare profile by selecting the central part using a 1.0-mm diameter pinhole (*P*) located on the excitation image plane of the microscope. The light then passes through the dichroic mirror (*DM*) and into a 63× air objective (*O*) to form a uniformly illuminated circular spot of 12 mm radius on the sample (*S*). Emitted light passes through the DM to reach the photomultiplier tube (*PMT*) (model #77345, Oriel Instruments, Strafford, CT). To avoid damage to the photocathode during bleaching, a third electronic shutter (*S1*) positioned before the PMT is closed during bleaching. Typical bleaching times are 40–100 ms. The light reflected from ND2 is collected and directed onto the sample to provide full-field illumination during visual inspection of large, homogeneous layers. An electronic shutter (*S4*) controls full-field illumination. The four electronic shutters and the PMT are interfaced with a personal computer (Dell Computer, Round Rock, TX) using an I/O board (PCI-MIO-E1, National Instruments, Austin, TX) and the graphical user interface program LabVIEW (National Instruments). Sample temperature is controlled with an aluminum plate (*TS*) connected to a circulating waterbath. For the sake of clarity, PMT, O, and TS are omitted from the top view, whereas W, M2, M4, ND1, ND2, S2, and S3 are omitted from the front view. Note that P, DM, O, S, TS, S1, and PMT are part of the epifluorescence microscope, not represented.

removing the proteins from CLSE. Prior studies have shown that the composition of phospholipid headgroups in the two preparations is the same (Hall et al., 1994). Measurements here with gas-liquid chromatography confirmed that the distribution of acyl chains in CLSE and N&PL were also unchanged (Fig. 2). Differences in the six dominant acyl chains (95% of the total) between CLSE and N&PL were minimal. The two preparations differed only in their content of protein, which fell in N&PL to undetectable levels, $<5\%$ of the amount in CLSE.

For coexisting gel and liquid-crystal phases, NBD-DMPE and shorter acyl-chain analogs partition almost exclusively into the more disordered phase (King and Marsh, 1986; Bultmann et al., 1991; Schram et al., 1996). In phase-separated bilayers, the probe therefore diffuses within the liquid-crystal phase, but its behavior also reflects the presence of the gel phase in which it is insoluble. FRAP measures two variables. The diffusion coefficient of the probe, D, determined from the rate of fluorescence recovery, is sensitive to the presence of obstacles to its movement,

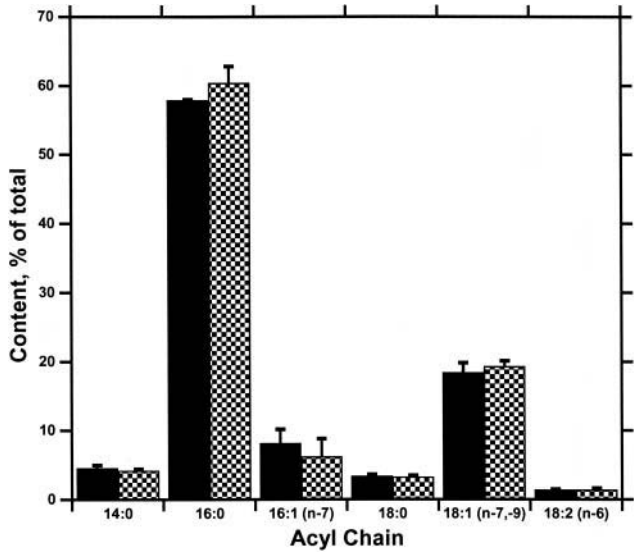

FIGURE 2 Composition of acyl chains in CLSE and N&PL. Methyl esters obtained from transmethylation of the complete preparations was analyzed by gas-liquid chromatography. The compounds shown represent the six most prevalent fatty acids, which together constituted >95% of the total. Data are mean values, with the error bars indicating the upper value of two measurements.

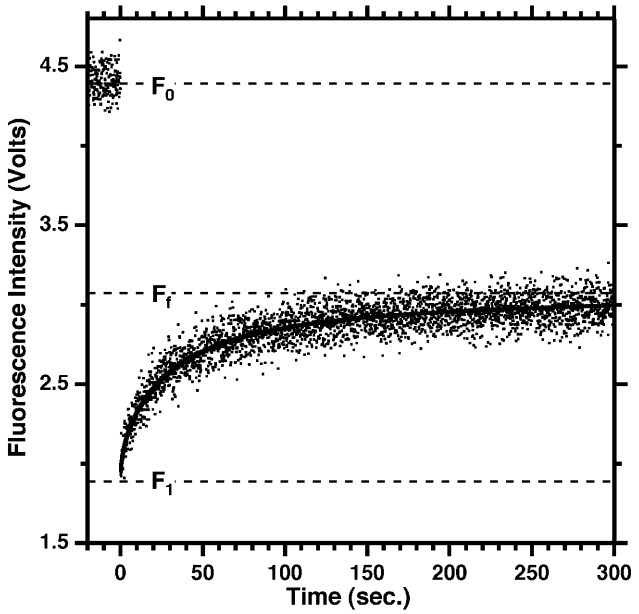

FIGURE 3 Response of fluorescence intensity to photobleaching. Samples contained CLSE multilayers with 0.5% NBD-DMPE (mol/mol). At time 0, a circular spot within the film was exposed to roughly even illumination with 488 nm light for 80 ms. Horizontal dashed lines indicate the fluorescence intensities, expressed as photomultiplier voltages, prior to photobleaching (F_0), immediately after photobleaching (F_1), and the predicted intensity after extrapolation to infinite time (F_f). The solid line provides the best fit to the experimental data during recovery of equations describing diffusion (see text). M, the mobile fraction, is obtained from $M = (F_f - F_1)/(F_0 - F_1)$.

including domains from which the probe is excluded. The mobile fraction, M, corresponding to the amount of probe that is free to diffuse, is determined from the extent of fluorescence recovery and should be 100% in an homogeneous liquid-crystalline membrane. In a bilayer with coexisting gel and liquid-crystal phases, M falls below 100% when enough gel phase is present to disconnect the fluid phase into isolated domains so that diffusion of the probe is restricted (Bultmann et al., 1991; Saxton, 1992; Schram et al., 1996). FRAP therefore provides information on phase separation as well as the rheology of the fluid phase.

Recovery traces for all of our bilayers fit well with previously published equations for diffusion described by a single value of D (Fig. 3). Results with multilayers containing a single phospholipid agreed with prior reports. For DOPC, values of D, which at 20°C was 5.3 ± 0.5 $\mu m^2/s$, agreed well with previously reported measurements (Vaz et al., 1985a), and showed the expected progressive increase at higher temperatures (Fig. 4). For DPPC, D dropped between 41 and 37°C by at least an order of magnitude from 11.7 ± 0.7 to 0.5 ± 0.3 $\mu m^2/s$, consistent with the gel-to-liquid crystal phase transition at 41°C (Fig. 4). At temperatures above 41°C, where both compounds occur as the disordered liquid-crystal phase, D for DPPC was significantly less than for DOPC, in agreement with previously reported values (Vaz et al., 1985b) (Fig. 4). M, the mobile fraction of the fluorescent probe, determined from the final fractional recovery of fluorescence intensity (Fig. 3), also agreed with behavior predicted from known phase behavior. As expected, M remained close to 1 for DOPC at all temperatures, and dropped dramatically for DPPC between 41° and 37°C (Fig. 5), coincident with the phase transition at 41°C.

Results with the complicated mixture of N&PL were similar to those for DOPC. Despite a composition that contains ~30% (mol/mol) of the fully saturated DPPC (Kahn et al., 1995; Uhlson et al., 2002), values of D were significantly higher for N&PL than for DPPC, and indistinguishable from those for DOPC (Fig. 4). This similarity extended over the full range of temperatures. M for N&PL remained close to 1 at all temperatures (Fig. 5), and so was also comparable to values for DOPC.

With the additional presence of the proteins in CLSE, behavior changed. Above 35°C, D for CLSE shifted to values below those not only for DOPC and N&PL, but also for DPPC in the range above 41°C at which that compound forms liquid-crystal bilayers. CLSE did not show the precipitous drop in D at lower temperatures that was evident for DPPC, but the temperature dependence of diffusion was greater below 35°C than at higher temperatures (Fig. 4).

Arrhenius plots detected this change around 35°C for CLSE as a discrete break in slope between linear segments at higher and lower temperatures (Fig. 6). Above 35°C, plots for CLSE were parallel to data for all other samples. The apparent activation energies, E'_a, defined as $-k\, d(\ln D)/d(1/$

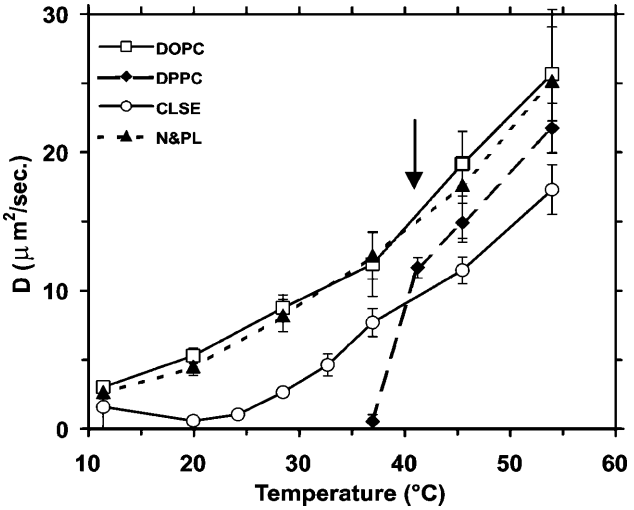

FIGURE 4 Translational diffusion coefficients of NBD-DMPE versus temperature in multilayers containing different compositions. Data are mean ± SD for 30 photobleaching experiments on each of three different samples. Arrow indicates the temperature (41°C) of the gel-to-liquid crystal phase transition for DPPC in calorimetric experiments.

T), for translational diffusion in this range of higher temperatures were therefore comparable for all samples at ~9.5 kcal/(°Kmole) (Table 1). This value was well within the range of values previously reported for NBD-DMPE diffusing in a fluid membrane (Schram and Thompson, 1995). Data for DOPC and N&PL fell along a single line at all temperatures, but for CLSE, the data fit different linear relationships above and below 35°C. At 11°C, where the slow rates and low fractional recoveries combined to produce the lowest signals, the single value of *D* fell well off the linear relationship and was ignored in further analysis.

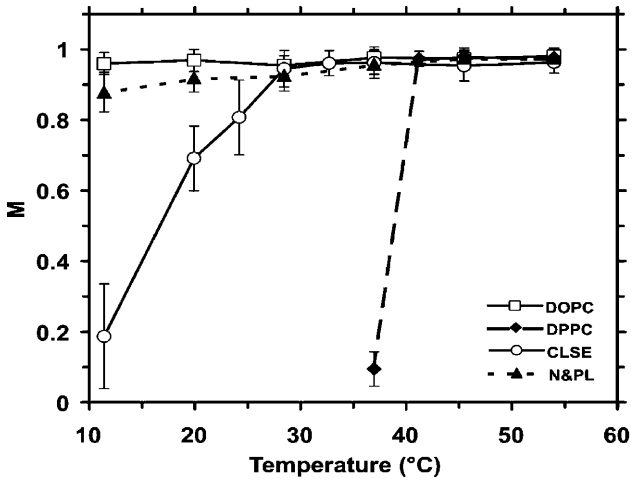

FIGURE 5 Mobile fractions of NBD-DMPE versus temperature on different multilayers. Data are mean ± SD for 30 photobleaching experiments on each of three different samples.

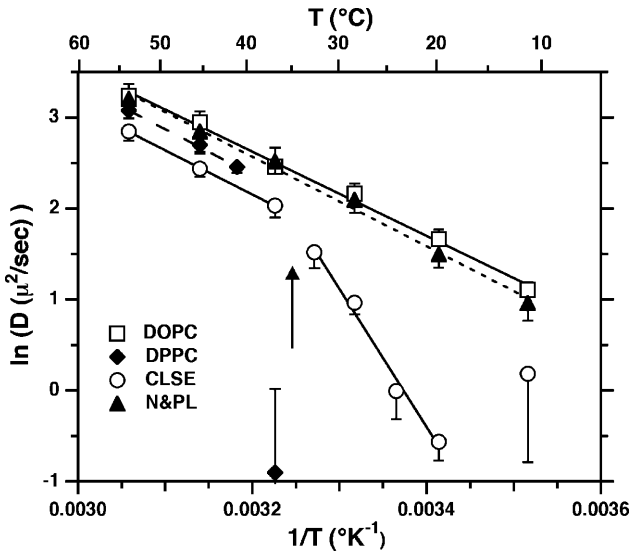

FIGURE 6 Arrhenius plots for diffusion coefficients of NBD-DMPE in multilayers with different compositions. Data are mean ± SD from 30 photobleaching experiments on each of three samples. Lines give best-fit linear regression to the data. Only points at temperatures above 41°C were fitted for DPPC. For CLSE, points above and below 35°C were adjusted separately, whereas the point at 11°C was ignored (see text). The arrow indicates the temperature (35°C) at which the two linear segments for CLSE intersect.

Extrapolated fits of the CLSE data for the two linear regions crossed at 35°C, suggesting a qualitative change in the multilayers at that point. For the data at lower temperature, higher values of E_a' (29.9 kcal/(°Kmole)) suggested that diffusion was restrained relative to behavior above 35°C by factors other than simply the reduction in thermal energy. The proteins also produced temperature-dependent changes in the mobile fraction for CLSE. Above 27°C, values approached 1 for all measurements, but at lower temperatures, *M* fell progressively, reaching 0.19 ± 0.14 at 11°C (Fig. 5). Although the rate of decline with falling temperature was less than the precipitous drop for DPPC, the behavior was in marked contrast to the constant values for N&PL without the proteins. The temperature dependence of *M* for CLSE was generally similar to that of *D*, but the break between the high and low temperature regions occurred at a lower temperature (27°C) than for *D* (35°C).

DISCUSSION

These studies address the effect of the hydrophobic surfactant proteins on diffusion within lipid bilayers. Rather than

TABLE 1 Apparent energies of activation for diffusion

	DOPC	DPPC	N&PL	CLSE, T < 35°C	CLSE, T > 35°C
E_a', kcal/(°K mole)	9.2	9.9	9.8	29.9	9.6

measuring changes caused by adding the purified proteins to individual lipids or simple mixtures, we instead report the effect of removing the proteins from complete surfactant extracts. This approach has the two advantages that our studies use the physiological mixture of surfactant lipids, and that we avoid the rapid loss of activity when SP-B and SP-C are separated from lipids (Cruz et al., 1997, 1998). The design of our studies does require that our protocol for removing the proteins must leave the lipids unaffected. Our group has shown previously that the composition of head groups and the content of cholesterol in CLSE and N&PL are indistinguishable (Hall et al., 1994). Here we also confirm that the composition of acyl groups is unchanged. Differences in diffusion between the two preparations must therefore result from removal of the proteins.

Our measurements of FRAP provide information on both the rheology and the phase behavior of pulmonary surfactant bilayers. Our studies focus on the effect of the hydrophobic surfactant proteins SP-B and SP-C, and compare the complete set of surfactant lipids (N&PL) alone and with the surfactant proteins (CLSE). Control experiments also determine the behavior of DOPC and of DPPC, and comparison of results for these bilayers with N&PL establishes the effect of lipids other than DPPC on the behavior of that major constituent. Our data for CLSE show two regions of temperature dependence distinguished by a break in Arrhenius plots at 35°C. We consider first the behavior of the lipids and then the different effects of the proteins at higher and lower temperatures.

Effect of lipids

Prior studies have shown that DOPC occurs as the liquid-crystal phase over the full range of temperatures considered here. Arrhenius plots for D are linear, but the basis of that linearity results only partially from the nature of diffusion (see Appendix). For a probe that diffuses freely on a lattice with diffusion coefficient D', the additional restriction that jumps occur only to neighboring sites with free area a_f sufficient to accommodate the molecule (Macedo and Litovitz, 1965; MacCarthy and Kozak, 1982; Almeida et al., 1992a) reduces the diffusion coefficient according to

$$D = D' \exp\left[-\frac{a_o}{a_f} - \frac{E_a}{kT}\right] \quad (1)$$

where a_o is the bilayer's close-packed molecular area, $a_f = a - a_o$ for a total molecular area a, and E_a is the activation energy for the jump. D' is also a function of temperature. For the range of temperatures considered here, however, ln D' is a linear function of $1/T$ (see Appendix). In the equation $D = A_o \exp(-E_a'/kT)$, the preexponential factor A_o is constant, the apparent activation energy, E_a', depends only on E_a and the thermal expansion coefficient α for the bilayer. The Arrhenius plots are therefore well behaved, and their slopes reflect E_a.

D is equivalent for DOPC and N&PL over the full range of temperatures. Values are significantly higher than for DPPC, including at temperatures above 41°C where that compound forms disordered liquid-crystal bilayers. Constituents in N&PL other than DPPC therefore significantly increase the fluidity of bilayers relative to DPPC alone. Although the other phospholipids are generally monoenoic or fully saturated compounds with melting transitions below the temperature for DPPC (Kahn et al., 1995), they shift D all the way to values for DOPC. The results generally fit with the original supposition (Notter, 1984; Keough, 1985) that despite the relatively high content of DPPC, the other lipids in pulmonary surfactant produce a fluid mixture.

Effect of proteins

The proteins have an effect opposite to that of the lipids other than DPPC. They slow diffusion in CLSE relative to N&PL over the full range of temperatures. At 35°C, the proteins in CLSE produce a change in the slope for the Arrhenius plots that is absent for N&PL. The plots for CLSE and N&PL are parallel above 35°C, but at lower temperatures, ln D falls more steeply for CLSE.

Below 35°C

The different slope below 35°C could theoretically result from changes in a_f or E_a (Eq. 1) or from the introduction of temperature-dependent obstacles to diffusion. Studies with binary systems favor obstacles consisting of a phase in which the probe is less soluble. For these binary mixtures, the change in temperature dependence coincides with the onset of phase coexistence detected by other methods. The effect of obstacles is given by $D^* = D/D_o$, where D_o is the diffusion coefficient in the absence of the obstacles, and D^* is a function of their size, shape, and concentration (Vaz et al., 1989; Almeida et al., 1992a; Saxton, 1994; Schram et al., 1994, 1996). Because

$$\ln D = \ln D^* + \ln D_o = \ln D^* + \ln A_o - \frac{E_a'}{kT} \quad (2)$$

obstacles that are invariant with respect to temperature, such as proteins, will shift an Arrhenius plot but leave its slope unaffected. Obstacles, however, formed by a new phase that grows during cooling will cause D^* to vary with temperature and so change the temperature dependence of D. The change in slope for the Arrhenius plots at 35°C is therefore consistent with the onset of phase separation in CLSE.

The change in M at 27°C provides further support that the proteins induce coexisting phases (Vaz et al., 1985a). The reduction in M indicates the presence of a percolation threshold at which the continuous phase breaks into discon-

tinuous domains (Saxton, 1982; Stauffer, 1985). For a probe soluble only in the discontinuous phase, the fraction that can participate in fluorescence recovery suddenly drops. The observed change in M requires a marked difference in the ability of the coexisting phases to accommodate the probe. Coexisting gel and liquid-crystal phases have the necessary characteristics. Phase separation must precede a percolation threshold, and so the change in M is expected at a temperature lower than the onset of coexistence. The behavior of M fits with the supposition that the change in D at 35°C reflects phase separation. The requirement by the low values of M that the probe is restricted by the new phase argues that the two phases are gel and liquid-crystal.

The results with pulmonary surfactant bilayers extend the information on phase behavior available from monolayers. At 20°C, compression of films containing both N&PL (Discher et al., 1999) and CLSE (Discher et al., 1996) initially induces separation of two phases. With further compression, however, both films remix immediately following a transition in the shape of the condensed domains that is characteristic of a critical point (Discher et al., 1999). In the presence of the proteins, phase separation in CLSE persists to higher surface pressures, reaching 35–40 mN/m, in contrast to N&PL, which remixed at 25–30 mN/m. Assuming a surface pressure in bilayers of ~35 mN/m (MacDonald, 1996), our results with multilayers are consistent with observations on monolayers. Although no phase separation is expected for N&PL in bilayers, the proteins elevate the critical point for CLSE to higher pressures, and so phase separation can occur.

Above 35°C

The Arrhenius plots for CLSE at higher temperatures are parallel to N&PL but shifted to lower values. The magnitude of the shift is particularly striking in light of the small amount of protein present. D for CLSE is 33–40% lower than for N&PL, below values for DPPC in the liquid-crystal phase, and yet the proteins represent only 1.5% (w/w) of the mixture. Assuming molecular areas of 540, 175, and 63 $Å^2$/molecule for SP-B, SP-C, and phospholipids in the liquid-crystal phase, respectively, and a 1:4 molar ratio between SP-B and SP-C (Perez-Gil et al., 1993; van Eijk et al., 1995), the proteins in CLSE should occupy $<1\%$ of the bilayer's surface area.

To the extent that the parallel slopes of the Arrhenius plots for the two preparations discriminate among possible mechanisms, the proteins should slow diffusion by creating temperature-independent obstacles. The shift to lower D without a change in slope requires that E_a' remain unaffected by the proteins, and suggests that they instead lower D^* in a temperature-independent manner. The proteins would produce the appropriate change in D^* if they themselves obstruct diffusion and retain roughly the same size, shape, and concentration during cooling. In light of their limited area, they are unable to explain the change in D^* if they occur as circular obstacles (Schram et al., 1994). Previous literature suggests that they may alter the mobility of neighboring lipid (Baatz et al., 1990; Vincent et al., 1991), but the observed reduction in D would require obstacles with a diameter ~20 lipid layers greater than for the proteins alone (Schram et al., 1994). The proteins could themselves act as obstacles sufficient to explain the lower D only if they form highly dendritic in-plane aggregates, but experimental support for this possibility is scarce. Fluorescence quenching experiments suggest that SP-B undergoes in-plane aggregation at the protein/phospholipids ratio in CLSE (Chang et al., 1998). SP-C has also been shown to self-associate, but mostly at temperatures below 38°C (Horowitz et al., 1993). The topology of the aggregates formed by SP-B and SP-C, however, remains unknown, and the extended configuration required to explain their effect on diffusion remains possible.

An alternative explanation of the reduced values of D is that the slopes of the Arrhenius plots are actually slightly different. The proteins would then produce a change in slope too small to detect over the narrow range of temperatures considered here, but large enough to shift D to lower values. Such an effect could result either from a change in E_a' or from a temperature-dependent D^*. If the proteins alter E_a', because the effect of a_f dominates E_a (Peters and Beck, 1983) they should do so by changing free area. A temperature-dependent D^* would occur if the proteins induce phase separation. At high temperatures in the presence of cholesterol, fully saturated phospholipids can form coexisting fluid phases (Ipsen et al., 1987). A more disordered liquid phase is continuous in the phase diagram with the liquid-crystal phase, but the liquid-ordered phase is distinct from the solid gel phase. The differences in solubility and rates of diffusion for the fluorescent probe are generally much less between the two fluid phases than for coexisting gel and liquid-crystal phases (Dietrich et al., 2001). Although less effective than gel-phase domains, regions of the liquid-ordered phase would nonetheless slow diffusion (Almeida et al., 1992b). The relative amounts of the two phases should vary during cooling, causing the variation of D^* and the different slope of the Arrhenius plots. The partial solubility of the probe in both phases would allow the apparent M to remain unaffected, consistent with our experimental results. In light of the phase behavior of similar systems and the difficulty of explaining the slower diffusion in terms of a direct effect, it remains possible that the proteins exert their influence indirectly by inducing liquid-liquid immiscibility.

Functional consequences

The present study tests the possibilities that the proteins might promote adsorption either by producing a more fluid bilayer or by creating interfacial boundaries. Our results

argue against both hypotheses. Contrary to early suggestions that all constituents other than DPPC promote fluidity, the proteins appear to have the opposite effect. At all temperatures, diffusion in the surfactant lipids becomes slower with the proteins rather than faster. The possibility of phase separation complicates interpretation. Below 35°C, the smaller values of D produced by the proteins reflect phase separation rather than a change in fluidity of the liquid phase. Above 35°C, however, the simplest interpretation of parallel Arrhenius plots is that CLSE, N&PL, DPPC, and DOPC all form uniformly liquid-crystal bilayers. The lower D in CLSE would then reflect changes in a homogeneous phase, and the inverse relationship between diffusion and viscosity would indicate that the proteins produce a more, rather than less, viscous bilayer.

The proteins do promote separation between gel and liquid-crystal phases, but not at physiological temperatures. Although the discontinuity that might promote bilayer fusion (Leckband et al., 1993) and interfacial adsorption (Gugliotti and Politi, 2001) does occur below 35°C, rates of adsorption show no change in their Arrhenius plots around that temperature (Schram and Hall, 2001). Our results reported here cannot exclude fluid-fluid phase separation for CLSE above 35°C. The introduction of the solid-fluid interface, however, at 35°C produces no discernable effect on adsorption at that temperature, and the reduced discontinuity expected between two fluid phases should have a smaller effect. Even if the proteins do cause immiscibility of fluid phases at 37°C, it seems unlikely that the effect explains their 10-fold acceleration of adsorption (Schram and Hall, 2001). Phase separation in bilayers could possibly lead to a more effective film at the interface. The observation that adsorbed films are remarkably stable at the beginning of the first compression in the lungs has suggested that the enrichment in DPPC stipulated by the classical model of surfactant function occurs by selective adsorption during the film's formation (Schürch et al., 1995). Separation induced by the proteins of ordered and disordered fluid phases would produce a presorting of DPPC in the bilayer (Brown and London, 2000). Although a thermodynamic or kinetic mechanism that would lead to preferential adsorption of the more ordered phase is still lacking, the segregation would at least provide a basis for selective insertion of the different compounds.

Both of the hypothetical mechanisms considered here, in which the proteins generate greater generalized or focal disorder, followed from initial thinking that factors which accelerate adsorption do so by destabilizing the surfactant vesicles. An alternative model contends instead that the proteins stabilize a rate-limiting structure intermediate between bilayer vesicle and interfacial monolayer (Walters et al., 2000; Schram and Hall, 2001). In arguing against a destabilizing effect, our results provide further support for the model in which the proteins act as an effective catalyst for promoting adsorption.

APPENDIX

Arrhenius behavior for diffusion in a homogenous bilayer

Analysis of our data in terms of Arrhenius plots requires some understanding of how diffusion should depend on temperature for a simple homogeneous bilayer. For a random walk on a square lattice of spacing λ, the diffusion coefficient D' is given by

$$D' = \frac{1}{4}\nu\lambda^2, \tag{A1}$$

where ν is the number of jumps per unit time (MacCarthy and Kozak, 1982). If each step represents an activated process in which the probe jumps only to adjacent free areas sufficiently large to accommodate the molecule, then modification of Eq. A.1 to account for the probability that the probe has sufficient energy and that the neighboring lattice site has sufficient free area yields

$$D = D' \exp\left(-\frac{a_o}{a_f} - \frac{E_a}{kT}\right), \tag{A2}$$

where a_o is the bilayer's close-packed area, the free area $a_f = a - a_o$, E_a is the energy of activation, k is the Boltzmann constant, and T is temperature (Macedo and Litovitz, 1965). If α, the thermal expansion coefficient, is constant, then a, the area, is given by

$$a = a_o + a_o\alpha(T - T_o), \tag{A3}$$

where T_o is the temperature at which the supercooled membrane would reach a_o (Galla et al., 1979; Clegg and Vaz, 1985). Then for $T \gg T_o$ (King and Marsh, 1986),

$$D = D' \exp\left(-\frac{1}{\alpha \mathrm{T}} - \frac{E_a}{kT}\right). \tag{A4}$$

Because both ν and λ depend on temperature, D' appears to vary during cooling, and equation A.4 indicates nonlinear Arrhenius plots for D. For

$$\nu = \frac{1}{\lambda}\left(\frac{2kT}{MW}\right)^{\frac{1}{2}}, \tag{A5}$$

where MW is molecular weight, then because $\lambda = a^{1/2}$, equations A.1, A.3, and A.5 yield

$$\ln D' = \frac{1}{2}\ln c + \frac{1}{2}\ln(T + \alpha T^2), \tag{A6}$$

where $c = (ka_o/8MW)$. Taylor series expansions, however, of $\ln(T + \alpha T^2)$ and $1/T$ indicate that for the range of temperatures considered, both functions vary linearly with temperature. Therefore

$$\ln(T + \alpha T^2) = \frac{m}{T} + b \tag{A7}$$

for constant m and b. Combination of equations A.4, A.6, and A.7 leads to

$$D = A_o\, e^{-\mathrm{E'_a/kT}}. \tag{A.8}$$

Arrhenius plots of D will be linear with intercept $A_o = (ce^b)^{1/2}$ and with constant slope yielding an ''apparent activation energy'' $E'_a = E_a + (k/\alpha) - (km/2)$.

The authors thank Dr. David Grainger of Colorado State University for helpful discussions and instrumental assistance, Dr. Edmund Egan of ONY for the gift of extracted calf surfactant, and Dr. William Connor and Linda

Bolewicz for assistance with gas chromatography. Walter Anyan prepared the samples of N&PL.

These studies were supported by the American Lung Association of Oregon, the Whitaker Foundation, and the National Institutes of Health (HL03502, HL54209, and a National Service Research Award).

REFERENCES

Almeida, P. F., W. L. Vaz, and T. E. Thompson. 1992a. Lateral diffusion and percolation in two-phase, two-component lipid bilayers. Topology of the solid-phase domains in-plane and across the lipid bilayer. *Biochemistry*. 31:7198–7210.

Almeida, P. F., W. L. Vaz, and T. E. Thompson. 1992b. Lateral diffusion in the liquid phases of dimyristoylphosphatidylcholine/cholesterol lipid bilayers: a free volume analysis. *Biochemistry*. 31: 6739–6747.

Ames, B. N. 1966. Assay of inorganic phosphate, total phosphate and phosphatases. *Methods Enzymol*. 8:115–118.

Arjomaa, P., and M. Hallman. 1988. Purification of a hydrophobic surfactant peptide using high-performance liquid chromatography. *Anal. Biochem*. 171:207–212.

Baatz, J. E., B. Elledge, and J. A. Whitsett. 1990. Surfactant protein SP-B induces ordering at the surface of model membrane bilayers. *Biochemistry*. 29:6714–6720.

Brown, D. A., and E. London. 2000. Structure and function of sphingolipid- and cholesterol-rich membrane rafts. *J. Biol. Chem*. 275:17221–17224.

Bultmann, T., W. L. Vaz, E. C. Melo, R. B. Sisk, and T. E. Thompson. 1991. Fluid-phase connectivity and translational diffusion in a eutectic, two-component, two-phase phosphatidylcholine bilayer. *Biochemistry*. 30:5573–5579.

Chang, R., S. Nir, and F. R. Poulain. 1998. Analysis of binding and membrane destabilization of phospholipid membranes by surfactant apoprotein B. *Biochim. Biophys. Acta*. 1371:254–264.

Clegg, R. M., and W. L. C. Vaz. 1985. Translational diffusion of proteins and lipids in artificial lipid bilayer membranes. *In* Progress in Protein-Lipid Interactions. A. Watts and J. J. H. H. M. de Pont, editors. Elsevier, Amsterdam. 173–229.

Cruz, A., C. Casals, K. M. W. Keough, and J. Perez-Gil. 1997. Different modes of interaction of pulmonary surfactant protein SP-B in phosphatidylcholine bilayers. *Biochem. J*. 327:133–138.

Cruz, A., C. Casals, I. Plasencia, D. Marsh, and J. Perez-Gil. 1998. Depth profiles of pulmonary surfactant protein B in phosphatidylcholine bilayers, studied by fluorescence and electron spin resonance spectroscopy. *Biochemistry*. 37:9488–9496.

Dietrich, C., L. A. Bagatolli, Z. N. Volovyk, N. L. Thompson, M. Levi, K. Jacobson, and E. Gratton. 2001. Lipid rafts reconstituted in model membranes. *Biophys. J*. 80:1417–1428.

Discher, B. M., K. M. Maloney, D. W. Grainger, C. A. Sousa, and S. B. Hall. 1999. Neutral lipids induce critical behavior in interfacial monolayers of pulmonary surfactant. *Biochemistry*. 38:374–383.

Discher, B. M., K. M. Maloney, W. R. Schief, Jr., D. W. Grainger, V. Vogel, and S. B. Hall. 1996. Lateral phase separation in interfacial films of pulmonary surfactant. *Biophys. J*. 71:2583–2590.

Galla, H. J., W. Hartmann, U. Theilen, and E. Sackmann. 1979. On two-dimensional passive random walk in lipid bilayers and fluid pathways in biomembranes. *J. Membr. Biol*. 48:215–236.

Gugliotti, M., and M. J. Politi. 2001. The role of the gel <=> liquid-crystalline phase transition in the lung surfactant cycle. *Biophys. Chem*. 89:243–251.

Hall, S. B., Z. Wang, and R. H. Notter. 1994. Separation of subfractions of the hydrophobic components of calf lung surfactant. *J. Lipid Res*. 35:1386–1394.

Hawgood, S., B. J. Benson, J. Schilling, D. Damm, J. A. Clements, and R. T. White. 1987. Nucleotide and amino acid sequences of pulmonary surfactant protein SP 18 and evidence for cooperation between SP 18 and SP 28–36 in surfactant lipid adsorption. *Proc. Natl. Acad. Sci. USA*. 84:66–70.

Horowitz, A. D., J. E. Baatz, and J. A. Whitsett. 1993. Lipid effects on aggregation of pulmonary surfactant protein SP-C studied by fluorescence energy transfer. *Biochemistry*. 32:9513–9523.

Ipsen, J. H., G. Karlstrom, O. G. Mouritsen, H. Wennerstrom, and M. J. Zuckermann. 1987. Phase equilibria in the phosphatidylcholine-cholesterol system. *Biochim. Biophys. Acta*. 905:162–172.

Kahn, M. C., G. J. Anderson, W. R. Anyan, and S. B. Hall. 1995. Phosphatidylcholine molecular-species of calf lung surfactant. *Am. J. Physiol.-Lung Cell. Mol. Physiol*. 13:L567–L573.

Kaplan, R. S., and P. L. Pedersen. 1989. Sensitive protein assay in presence of high levels of lipid. *Methods Enzymol*. 172:393–399.

Keough, K. M. W. 1985. Lipid fluidity and respiratory distress syndrome. *In* Membrane Fluidity in Biology. Vol. 3. Disease Processes. R. C. Aloia and J. M. Boggs, editors. Academic Press, Orlando, FL. 39–84.

King, M. D., and D. Marsh. 1986. Free volume model for lipid lateral diffusion coefficients. Assessment of the temperature dependence in phosphatidylcholine and phosphatidylethanolamine bilayers. *Biochim. Biophys. Acta*. 862:231–234.

Lardner, T. J. 1977. The measurement of cell membrane diffusion coefficients. *J. Biomech*. 10:167–170.

Leckband, D. E., C. A. Helm, and J. Israelachvili. 1993. Role of calcium in the adhesion and fusion of bilayers. *Biochemistry*. 32:1127–1140.

Lopez, A., L. Dupou, A. Altibelli, J. Trotard, and J. F. Tocanne. 1988. Fluorescence recovery after photobleaching (FRAP) experiments under conditions of uniform disk illumination. Critical comparison of analytical solutions, and a new mathematical method for calculation of diffusion coefficient D. *Biophys. J*. 53:963–970.

MacCarthy, J. E., and J. J. Kozak. 1982. Lateral diffusion in fluid systems. *J. Chem. Phys*. 77:2214–2216.

MacDonald, R. C. 1996. The relationship and interactions between lipid bilayer vesicles and lipid monolayers at the air/water interface. *In* Vesicles. M. Rosoff, editor. Marcel Dekker, New York. 1–48.

Macedo, P. B., and T. A. Litovitz. 1965. On the relative roles of free volume and activation energy in the viscosity of liquids. *J. Chem. Phys*. 42:245–256.

Nogee, L. M. 1998. Genetics of the hydrophobic surfactant proteins. *Biochim. Biophys. Acta*. 1408:323–333.

Notter, R. H. 1984. Surface chemistry of pulmonary surfactant: the role of individual components. *In* Pulmonary Surfactant. B. Robertson, L. M. G. van Golde, and J. J. Batenburg, editors. Elsevier, Amsterdam. 17–64.

Notter, R. H., J. N. Finkelstein, and R. D. Taubold. 1983. Comparative adsorption of natural lung surfactant, extracted phospholipids, and artificial phospholipid mixtures to the air-water interface. *Chem. Phys. Lipids*. 33:67–80.

Oosterlaken-Dijksterhuis, M. A., H. P. Haagsman, L. M. G. van Golde, and R. A. Demel. 1991. Interaction of lipid vesicles with monomolecular layers containing lung surfactant proteins SP-B or SP-C. *Biochemistry*. 30:8276–8281.

Perez-Gil, J., A. Cruz, and C. Casals. 1993. Solubility of hydrophobic surfactant proteins in organic solvent/water mixtures. Structural studies on SP-B and SP-C in aqueous organic solvents and lipids. *Biochim. Biophys. Acta*. 1168:261–270.

Peters, R., and K. Beck. 1983. Translational diffusion in phospholipid monolayers measured by fluorescence microphotolysis. *Proc. Natl. Acad. Sci. USA*. 80:7183–7187.

Saxton, M. J. 1982. Lateral diffusion in an archipelago. Effects of impermeable patches on diffusion in a cell membrane. *Biophys. J*. 39: 165–173.

Saxton, M. J. 1992. Lateral diffusion and aggregation. A Monte Carlo study. *Biophys. J*. 61:119–128.

Saxton, M. J. 1994. Anomalous diffusion due to obstacles. A Monte Carlo study. *Biophys. J*. 66:394–401.

Schram, V., and S. B. Hall. 2001. Thermodynamic effects of the hydrophobic surfactant proteins on the early adsorption of pulmonary surfactant. *Biophys. J.* 81:1536–1546.

Schram, V., H. N. Lin, and T. E. Thompson. 1996. Topology of gel-phase domains and lipid mixing properties in phase-separated two-component phosphatidylcholine bilayers. *Biophys. J.* 71:1811–1822.

Schram, V., and T. E. Thompson. 1995. Interdigitation does not affect translational diffusion of lipids in liquid crystalline bilayers. *Biophys. J.* 69:2517–2520.

Schram, V., J. F. Tocanne, and A. Lopez. 1994. Influence of obstacles on lipid lateral diffusion: computer simulation of FRAP experiments and application to proteoliposomes and biomembranes. *Eur. Biophys. J.* 23:337–348.

Schürch, S., R. Qanbar, H. Bachofen, and F. Possmayer. 1995. The surface-associated surfactant reservoir in the alveolar lining. *Biol. Neonate.* 67(Suppl. 1):61–76.

Searcy, R. L., and L. M. Bergquist. 1960. A new color reaction for the quantitation of serum cholesterol. *Clin. Chim. Acta.* 5:192–199.

Soumpasis, D. M. 1983. Theoretical analysis of fluorescence photobleaching recovery experiments. *Biophys. J.* 41:95–97.

Stauffer, D. 1985. Introduction to Percolation Theory. Taylor & Francis, London.

Tokieda, K., J. A. Whitsett, J. C. Clark, T. E. Weaver, K. Ikeda, K. B. McConnell, A. H. Jobe, M. Ikegami, and H. S. Iwamoto. 1997. Pulmonary dysfunction in neonatal SP-B-deficient mice. *Am. J. Physiol.* 273:L875–L882.

Uhlson, C., K. Harrison, C. B. Allen, S. Ahmad, C. W. White, and R. C. Murphy. 2002. Oxidized phospholipids derived from ozone-treated lung surfactant extract reduce macrophage and epithelial cell viability. *Chem. Res. Toxicol.* 15:896–906.

van Eijk, M., C. G. De Haas, and H. P. Haagsman. 1995. Quantitative analysis of pulmonary surfactant proteins B and C. *Anal. Biochem.* 232:231–237.

Vaz, W. L., R. M. Clegg, and D. Hallmann. 1985a. Translational diffusion of lipids in liquid crystalline phase phosphatidylcholine multibilayers. A comparison of experiment with theory. *Biochemistry.* 24:781–786.

Vaz, W. L., D. Hallmann, R. M. Clegg, A. Gambacorta, and M. De Rosa. 1985b. A comparison of the translational diffusion of a normal and a membrane-spanning lipid in L alpha phase 1-palmitoyl-2-oleoylphosphatidylcholine bilayers. *Eur. Biophys. J.* 12:19–24.

Vaz, W. L., E. C. Melo, and T. E. Thompson. 1989. Translational diffusion and fluid domain connectivity in a two-component, two-phase phospholipid bilayer. *Biophys. J.* 56:869–876.

Vaz, W. L. 1994. Diffusion and chemical reactions in phase-separated membranes. *Biophys. Chem.* 50:139–145.

Vincent, J. S., S. D. Revak, C. G. Cochrane, and I. W. Levin. 1991. Raman spectroscopic studies of model human pulmonary surfactant systems: phospholipid interactions with peptide paradigms for the surfactant protein SP-B. *Biochemistry.* 30:8395–8401.

Walters, R. W., R. R. Jenq, and S. B. Hall. 2000. Distinct steps in the adsorption of pulmonary surfactant to an air-liquid interface. *Biophys. J.* 78:257–266.

Wang, Z., S. B. Hall, and R. H. Notter. 1996. Roles of different hydrophobic constituents in the adsorption of pulmonary surfactant. *J. Lipid Res.* 37:790–798.

Warr, R. G., S. Hawgood, D. I. Buckley, T. M. Crisp, J. Schilling, B. J. Benson, P. L. Ballard, J. A. Clements, and R. T. White. 1987. Low molecular weight human pulmonary surfactant protein (SP5): isolation, characterization, and cDNA and amino acid sequences. *Proc. Natl. Acad. Sci. USA.* 84:7915–7919.

Whitsett, J. A., B. L. Ohning, G. Ross, J. Meuth, T. Weaver, B. A. Holm, D. L. Shapiro, and R. H. Notter. 1986. Hydrophobic surfactant-associated protein in whole lung surfactant and its importance for biophysical activity in lung surfactant extracts used for replacement therapy. *Pediatr. Res.* 20:460–467.

Yu, S. H., and F. Possmayer. 1990. Role of bovine pulmonary surfactant-associated proteins in the surface-active property of phospholipid mixtures. *Biochim. Biophys. Acta.* 1046:233–241.